


The globular cluster VVV CL002 falling down to the hazardous Galactic centre

Dante Minniti^{1,2,3} , Noriyuki Matsunaga^{4,5}, José G. Fernández-Trincado⁶, Shogo Otsubo⁵, Yuki Sarugaku⁵, Tomomi Takeuchi⁵, Haruki Katoh⁵, Satoshi Hamano⁷, Yuji Ikeda^{5,8}, Hideyo Kawakita^{5,9}, Philip W. Lucas¹⁰, Leigh C. Smith¹¹, Iaria Petralia¹, Elisa Rita Garro¹, Roberto K. Saito³, Javier Alonso-García¹², Matías Gómez¹, and María Gabriela Navarro¹³

¹ Instituto de Astrofísica, Depto. de Ciencias Físicas, Facultad de Ciencias Exactas, Universidad Andres Bello, Fernandez Concha 700, Santiago, RM, Chile
e-mail: dante.minniti@unab.cl

² Specola Vaticana, Vatican Observatory, Castelgandolfo, V00120 Stato Citta Vaticano, Italy

³ Departamento de Física, Universidade Federal de Santa Catarina, Florianopolis, Trindade 88040-900, SC, Brazil

⁴ Department of Astronomy, School of Science, The University of Tokyo, 7-3-1 Hongo, Bunkyo-ku, Tokyo 113-0033, Japan
e-mail: matsunaga@astron.s.u-tokyo.ac.jp

⁵ Laboratory of Infrared High-resolution Spectroscopy (LiH), Koyama Astronomical Observatory, Kyoto Sangyo University, Motoyama, Kamigamo, Kita-ku, Kyoto 603-8555, Japan

⁶ Instituto de Astronomía, Universidad Católica del Norte, Av. Angamos 0610, Antofagasta, Chile

⁷ National Astronomical Observatory of Japan, 2-21-1 Osawa, Mitaka, Tokyo 181-8588, Japan

⁸ Photocoding, 460-102 Iwakura-Nakamachi, Sakyo-ku, Kyoto 606-0025, Japan

⁹ Department of Astrophysics and Atmospheric Sciences, Faculty of Science, Kyoto Sangyo University, Motoyama, Kamigamo, Kita-ku, Kyoto 603-8555, Japan

¹⁰ Centre for Astrophysics Research, University of Hertfordshire, College Lane, Hatfield AL10 9A, UK

¹¹ Institute of Astronomy, University of Cambridge, Madingley Rd., Cambridge CB3 0HA, UK

¹² Centro de Astronomía (CITEVA), Universidad de Antofagasta, Av. Angamos 601, Antofagasta, Chile

¹³ INAF, Osservatorio Astronomico di Roma, Via di Frascati 33, Monteporzio Catone 00040, Italy

Received 28 September 2023 / Accepted 11 December 2023

ABSTRACT

Context. The Galactic centre is hazardous for stellar clusters because of the strong tidal force in action there. It is believed that many clusters were destroyed there and contributed stars to the crowded stellar field of the bulge and the nuclear stellar cluster. However, the development of a realistic model to predict the long-term evolution of the complex inner Galaxy has proven difficult, and observations of surviving clusters in the central region would provide crucial insights into destruction processes.

Aims. Among the known Galactic globular clusters, VVV CL002 is the closest to the centre, at 0.4 kpc, but has a very high transverse velocity of 400 km s⁻¹. The nature of this cluster and its impact on Galactic astronomy need to be addressed with spectroscopic follow up.

Methods. Here we report the first measurements of its radial velocity and chemical abundance based on near-infrared high-resolution spectroscopy.

Results. We find that this cluster has a counter-rotating orbit constrained within 1.0 kpc of the centre, and as close as 0.2 kpc at the perigalacticon, confirming that the cluster is not a passerby from the halo but a genuine survivor enduring the harsh conditions of the tidal forces of the Galactic mill. In addition, its metallicity and α abundance ($[\alpha/\text{Fe}] \simeq +0.4$ and $[\text{Fe}/\text{H}] = -0.54$) are similar to those of some globular clusters in the bulge. Recent studies suggest that stars with such α -enhanced stars were more common at 3–6 kpc from the centre around 10 Gyr ago.

Conclusions. We infer that VVV CL002 was formed outside but is currently falling down to the centre, showcasing a real-time event that must have occurred to many clusters a long time ago.

Key words. stars: abundances – globular clusters: general – Galaxy: nucleus

1. Introduction

Although more than 200 globular clusters have been found to exist today in the Galaxy, there is plenty of evidence suggesting that many others have been destroyed by various evolutionary and dynamical processes, including dynamical friction, shocking by disk and bulge, tidal disruption, and so on (Leon et al. 2000; Murali & Weinberg 1997; Gnedin & Ostriker 1997; Baumgardt & Makino 2003; Moreno et al. 2022). A sig-

nificant number of these dynamical processes are stronger in the deep potential well of the inner Galaxy. Numerical simulations have revealed that the supermassive black hole Sagittarius A* (Ghez et al. 2008; Genzel et al. 2010) can very efficiently grind clusters, and is a place where globular clusters could be rapidly demolished (Arca-Sedda & Capuzzo-Dolcetta 2017; Navarro et al. 2023). In order to address the process of globular-cluster disruption, it is crucial to understand not only clusters that have been destroyed but also surviving globular

clusters. Searches for globular clusters in the inner Galaxy are incomplete because of high levels of interstellar extinction and heavy source crowding. Still, recent near-infrared (NIR) surveys have revealed dozens of candidate clusters in the inner bulge (Moni Bidin et al. 2011; Borissova et al. 2014). Nevertheless, confirmation of member stars and detailed characterisation of cluster properties require infrared spectroscopic observations due to the high level of interstellar extinction near the centre.

VVV CL002 is a relatively low-luminosity globular cluster ($M_K = -7.1$ mag, $M_V = -4.6$ mag, Minniti et al. 2021) discovered at 1.1 deg from the Galactic centre during the VISTA Variables in the Via Lactea (VVV) survey (Moni Bidin et al. 2011). The distance measured with the red clump places VVV CL002 at the closest point to the centre of any known cluster, at 0.4 kpc, and an additional surprise is its high transverse velocity, of namely 400 km^{-1} , which was inferred from the proper motion (PM) (Minniti et al. 2021). Some RR Lyr variables with such high velocities found in the bulge were later found to be halo objects (Kunder et al. 2020). Whether or not VVV CL002 is an interloper from the halo passing near the Galactic centre remains unclear. If, instead, it remains near the centre, we need to consider how it is surviving without being tidally disrupted. Spectroscopic observations are required to answer these questions.

2. Observation and data analysis

2.1. Target selection

As VVV CL002 is embedded in the crowded stellar field, selecting good targets for follow-up spectroscopic observations is a crucial step. In particular, cluster membership determination is very difficult in such a crowded field (Fig. 1). The line-of-sight contamination of stars in various groups increases at low latitudes, and accurate 6D information (position, radial velocity, and PM) is vital to judging membership. Based on the VVV photometry and PMs in the updated VIRAC2 database (Smith et al., in prep.), we selected a few candidate red giant branch (RGB) candidates (Fig. 2), including the two stars that we finally observed. To this end, we initially selected the four brightest RGB stars with high probability of membership according to the photometric and astrometric data. The main criteria for the selection of this sample were: (1) Stars within 0.1 mag of the mean RGB ridge line in the NIR colour–magnitude diagram (CMD); (2) stars with PMs within 0.1 mas yr^{-1} from the mean GC PM; (3) stars that appeared unblended in the optical and NIR images; and (4) stars brighter than $J = 14.2$ mag. Two out of these four main selected targets were successfully observed (Table 1). The remaining two targets could not be observed due to time and weather constraints during our observing run. These are *Gaia* ID 9327562004074, with $K_s = 11.87$ mag and $J - K_s = 2.22$ mag; and *Gaia* ID 9327562025638, with $K_s = 11.90$ mag and $J - K_s = 2.24$ mag, which would also be prime targets for future spectroscopic observations. The PMs of candidate members of VVV CL002 show a large offset from the bulk of bulge field stars, which indicates the large transverse velocity of the clusters, of namely $\sim 400 \text{ km s}^{-1}$ (Minniti et al. 2021). Although some contaminants remain, stars selected by the PM show the RGB and red clump expected for a globular cluster.

2.2. Observation

On June 10, 2023, we used the WINERED spectrograph (Ikeda et al. 2022; Matsunaga et al. 2023) attached to the Magellan Clay telescope in Chile to obtain high-



Fig. 1. Near-infrared image of the field around VVV CL002 made with VVV images in the JHK_s -band filters, indicating the target red giant stars A (VIRAC2 ID=9327562027332) and B (VIRAC2 ID=9327562015390). The field covers $4' \times 3'$, oriented along Galactic coordinates, with latitude increasing upwards and longitude to the left. The globular cluster is located at the centre of this image, which also illustrates the overwhelming density of field stars.

resolution spectra of VIRAC2 ID=9327562027332 and VIRAC2 ID=9327562015390. WINERED is a NIR high-resolution spectrograph covering $0.90\text{--}1.35 \mu\text{m}$ (z' , Y , and J bands), with a resolution of $R = \lambda/\Delta\lambda = 28\,000$ with the WIDE mode (Ikeda et al. 2022). The raw spectral data were reduced with the WINERED Automatic Reduction Pipeline (WARP¹, version 3.8). We confirmed that the broadening width in the final spectra is as small as 12 km s^{-1} , which can be explained by the combination of the instrumental resolution (10.7 km s^{-1}) and a typical macroturbulence of about 5 km s^{-1} . These stars at $J \approx 13.5$ mag are the brightest among a few targets that were selected as candidate members. However, at this magnitude they are still challenging for high-resolution spectroscopy in the infrared, and our spectra – with 1200 s exposures for each star – are of moderate quality. While the signal-to-noise ratios are $S/N = 30\text{--}50$ in the J band, they are 15–20 in the Y band (shorter wavelengths) because of severe interstellar extinction. Therefore, our analysis relied mainly on the J -band part of the spectra (Fig. 3). The spectra of the two stars show a striking resemblance to each other (Fig. 3), with the same absorption lines appearing at the same wavelengths and exhibiting very similar depths. This already indicates that the two target stars are red giants with very similar characteristics, belonging to a common stellar group, VVV CL002.

2.3. Measurements of radial velocities

We measured radial velocities using the cross-correlation technique, involving the model synthetic spectra and telluric absorption spectra (Matsunaga et al. 2015). For this analysis, we include some Y -band echelle orders together with J -band orders, in which telluric lines and stellar lines are well mixed. We obtained almost identical velocities for the two stars (Table 1), strongly supporting the membership to VVV CL002 combined with the PMs (Fig. 2).

¹ <https://github.com/SatoshiHamano/WARP/>

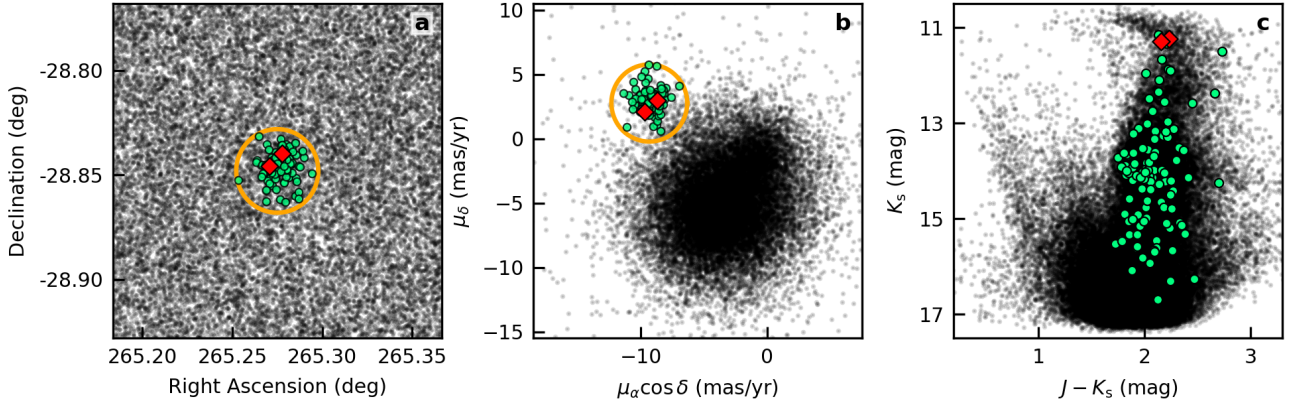


Fig. 2. Illustration of the target selection from VVV CL002. Panel a: field surrounding the cluster, panel b: proper motion diagram. Panel c: NIR colour–magnitude diagram. The field stars are plotted with the black points, while stars located inside the selection circles (orange) in panels a and b are indicated by green circles. Some of these stars in green were selected as spectroscopic targets based on panel c, and we observed the two red giants indicated by red diamonds.

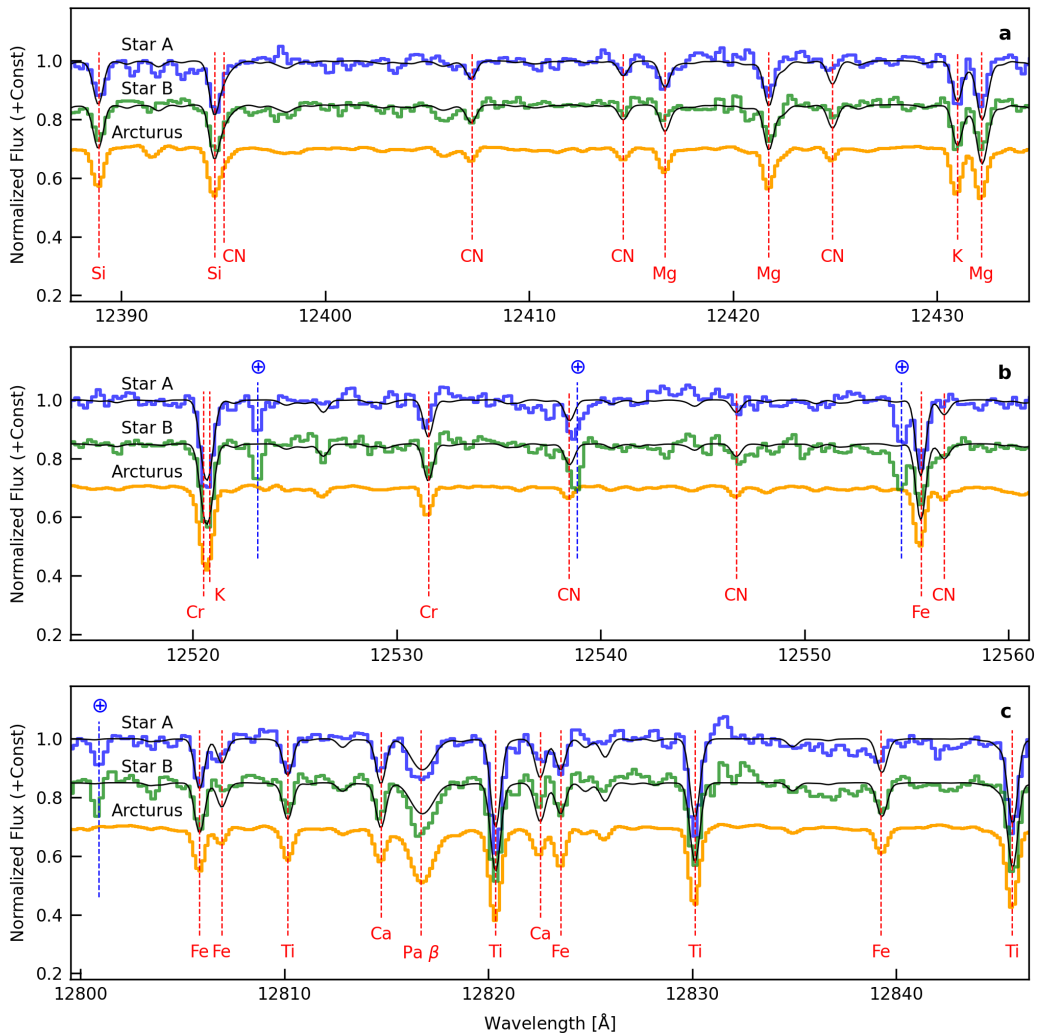
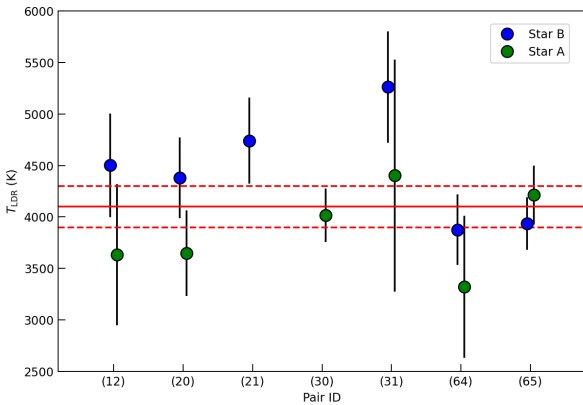


Fig. 3. Spectra for the two red giant members of the globular cluster VVV CL002. Star A (VIRAC2 ID=9327562027332) is shown in blue and star B (VIRAC2 ID=9327562015390) in green. Three representative parts containing absorption lines used for abundance measurements (Mg, Si, and Fe) and other lines are presented together with model spectra synthesized with $T_{\text{eff}} = 4100$ K, $\log g = 1.5$, and $[\text{Fe}/\text{H}] = -0.54$ (black). The spectrum of Arcturus (orange) is also shown for comparison, shifted to the appropriate velocity to match the spectra of the target stars. Arcturus ($T_{\text{eff}} = 4280$ K, $[\text{Mg}/\text{H}] = -0.2$, $[\text{Si}/\text{H}] = -0.2$, $[\text{Fe}/\text{H}] = -0.5$) is a prototype red giant observed with the same setup (Fukue et al. 2021). We note that all the spectra appear very similar to each other. Absorption lines marked \oplus are telluric lines, which are only seen in the two target stars but not in Arcturus for which a telluric correction was performed.

Table 1. Observed target stars and mean globular cluster parameters.

Parameter	Star A	Star B	Mean
ID (VIRAC2)	9327562027332	9327562015390	
RA (J2000)	17:41:06.65	17:41:04.94	
Dec (J2000)	-28:50:23.1	-28:50:44.4	
K_s (mag)	11.25	11.21	
$J - K_s$ (mag)	2.20	2.25	
V_{helio} (km s $^{-1}$)	-27.3 ± 0.2	-27.3 ± 0.2	-27.3 ± 0.1
V_{LSR} (km s $^{-1}$)	-17.0 ± 0.2	-17.1 ± 0.2	-17.1 ± 0.1
[Fe/H]	-0.68 ± 0.37	-0.39 ± 0.41	-0.54 ± 0.27
[Mg/H]	-0.26 ± 0.19	-0.14 ± 0.12	-0.19 ± 0.10
[Si/H]	-0.12 ± 0.29	-0.02 ± 0.25	-0.07 ± 0.19

**Fig. 4.** Spectroscopic line-depth ratio temperatures estimated with line pairs taken from Taniguchi et al. (2018). The solid and dashed lines indicate the temperature and its error used for measuring the chemical abundances of the two stars.

2.4. Measurements of chemical abundances

In spite of the limited S/N, we are able to measure the abundances of Fe, Mg, and Si. First, we estimated the effective temperature based on line-depth ratios (Taniguchi et al. 2018). We were able to measure the ratios of 6–7 line pairs taken from Taniguchi et al. (2018) as illustrated in Fig. 4. Adopting an error of 200 K, we use the approximate value of the temperatures, $T_{\text{eff}} = 4100$ K, for both stars in the following analysis. It is impossible to determine other stellar parameters due to the limited quality of the current spectra. Considering the similarity to Arcturus, we used the following parameters: $\log g = 1.5$, and the microturbulent velocity $\xi = 1.5$ km s $^{-1}$ (Fukue et al. 2021).

We then determined the chemical abundances by fitting model spectra to individual absorption lines isolated from telluric lines and other strong stellar lines. Measurements were successfully obtained for about ten Fe I lines, seven Si lines, and four Mg lines, leading to the abundances listed in Table 1. The errors in the [X/H] values for individual stars are given by the combination of the standard deviations of the line-by-line abundances and the systematic errors caused by uncertainties in stellar parameters such as T_{eff} . The line-by-line random errors dominate the total errors in all cases; that is, the three elements in the two stars. Among the systematic errors, that from the $\log g$ uncertainty tends to be the largest source of error, of namely 0.6–0.9 dex in [X/H], but the T_{eff} uncertainty has the highest impact on [Si/H], of namely ~ 0.1 dex. The trends in the systematic errors are similar to those found for Arcturus (Fig. 7 in Fukue et al. 2021), but the errors in each stellar parameter,

especially $\log g$, are significantly larger for our targets. Finally, we took weighted means and their errors of the [X/H] values of the two stars to discuss the chemical abundances of the cluster (Table 1). We obtained almost identical velocities and common chemical abundances within the errors for the two stars (Table 1). Such close agreement is unexpected for field stars in the bulge characterised by a large velocity dispersion and a wide metallicity distribution (Recio-Blanco 2018; Zasowski et al. 2019; Schultheis et al. 2020; Geisler et al. 2021; Queiroz et al. 2021). In addition, the spectra of these two stars are similar to the high-S/N spectrum of the prototype red giant Arcturus ([Mg/H] = -0.2 , [Si/H] = -0.2 , [Fe/H] = -0.5 ; Fukue et al. 2021), supporting the metallicities and the α enhancement of our two stars. There are absorption lines of some other elements seen in the obtained spectra, as indicated in Fig. 1. It would be valuable to measure the abundances of such elements, but we limited ourselves to the three elements (Fe, Si, and Mg) for which a simple analysis with the limited-S/N spectra was sufficient. For example, the number of useful Ca lines is more limited than those of Mg because of blends by telluric lines and stellar lines, and also because only a few lines have moderate depths with the limited S/N values. Ti tends to be affected by non local thermodynamic equilibrium. Measuring C and/or N abundances with CN would require CO and OH lines together, but none of these lines are available in the WINERED range.

3. Cluster orbit

We computed the orbit of VVV CL002 using the 3D barred Galaxy steady-state potential model of the GravPot16 code (Fernández-Trincado et al. 2022). We ran the orbital simulation considering different bar pattern speeds, $\Omega_{\text{bar}} = 31, 41,$ and 51 km s $^{-1}$ kpc $^{-1}$ (Sanders et al. 2019). For VVV CL002, we obtained 10000 orbits, adopting a simple Monte Carlo resampling, where the uncertainties in the input coordinates (α, δ), PMs, radial velocities, and distance errors were randomly propagated as 1σ variations in the Gaussian Monte Carlo resampling. Figure 5 shows the computed orbits using $\Omega_{\text{bar}} = 41$ km s $^{-1}$ kpc $^{-1}$, displayed as probability densities of orbits projected on the equatorial Galactic plane (left panel), and height above the plane z versus Galactocentric radius in kiloparsecs (right panel). The lighter colours indicate the more probable regions of space that are travelled more frequently by the simulated orbits. According to the result of this calculation, VVV CL002 has a retrograde orbital configuration of relatively high eccentricity ($e = 0.69 \pm 0.22$), with perigalactocentric and apogalactocentric distances well inside the Galactic bulge at $R_{\text{peri}} = 0.19 \pm 0.21$ kpc and $R_{\text{apo}} = 1.04 \pm 0.29$ kpc, respectively, and with moderate vertical excursions from the Galactic plane ($|z_{\text{max}}| = 0.35 \pm 0.09$ kpc). It is important to note that with any adopted heliocentric distance, our simulations confirm that, kinematically, VVV CL002 now belongs to the bulge, and is not merely a halo globular cluster in a very eccentric orbit passing by the inner bulge.

4. Discussion

The radial velocity we obtained allows us to put strong constraints on the full 3D motion of the cluster. We calculated 10000 orbits of VVV CL002 by adopting a Monte Carlo resampling with the uncertainties in input parameters, such as distance, radial velocity, and PM taken into account. We find that VVV CL002 has a retrograde orbital configuration of relatively high eccentricity ($e = 0.69 \pm 0.22$), with

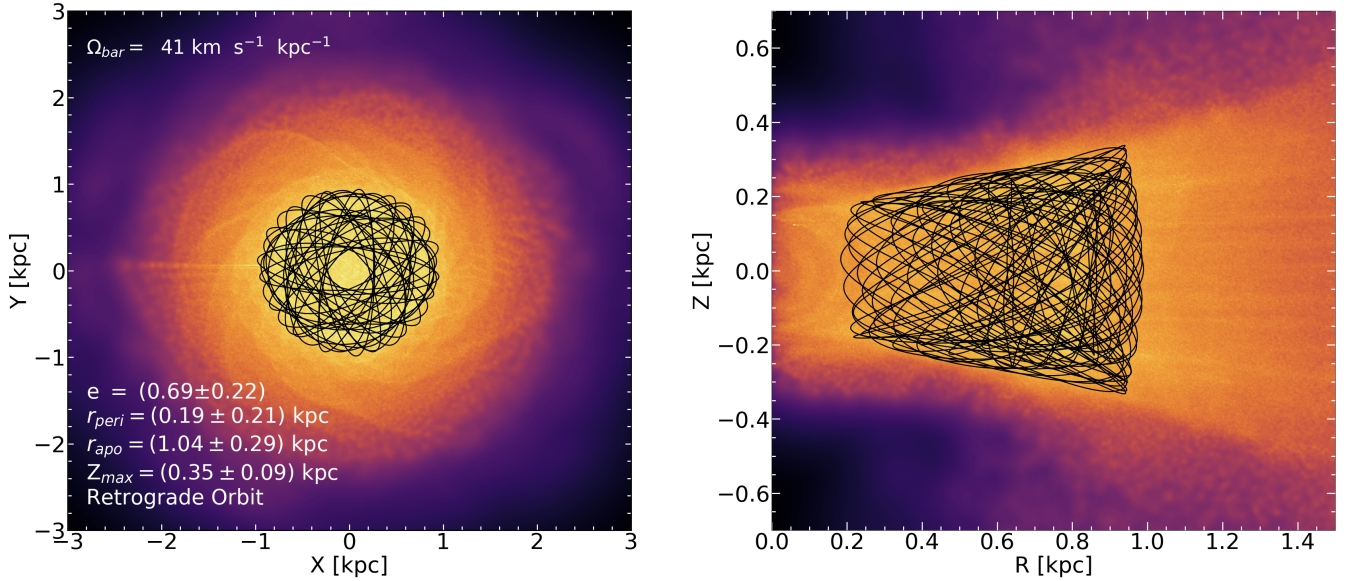


Fig. 5. Orbit computed for VVV CL002 (black line), overlaid on the probability densities of orbits projected on the Galactic plane (left) and height above the plane z versus Galactocentric radius (right). Lighter colours indicate more probable regions of space that are more frequently sampled by the simulated orbits.

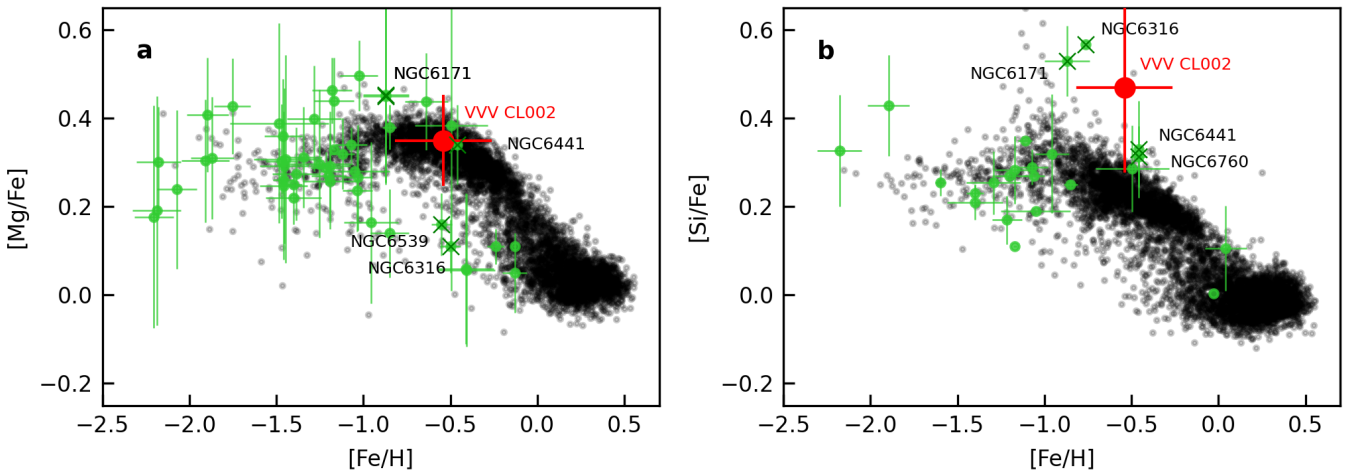


Fig. 6. $[\text{Mg}/\text{Fe}]$ versus $[\text{Fe}/\text{H}]$ (left) and $[\text{Si}/\text{Fe}]$ versus $[\text{Fe}/\text{H}]$ (right) for the globular cluster VVV CL002 (red circle) compared with the abundances of other known globular clusters indicated by green circles (Mészáros et al. 2020; Carretta et al. 2009; Dias et al. 2016; Recio-Blanco 2018; Barbay et al. 2018, 2021; Geisler et al. 2021; Schiavon et al. 2024) and bulge field stars indicated by small dots (Abdurro'uf 2022; Queiroz et al. 2023). The globular cluster mean abundances with their respective errors are all from mid- and high-resolution optical and IR spectroscopy from the literature as compiled by Garro et al. (2023). A few representative globular clusters that show abundances similar to those of VVV-CL002 are also marked with crosses and are labelled for comparison.

perigalactocentric and apogalactocentric distances of $R_{\text{peri}} = 0.19 \text{ kpc}$ and $R_{\text{apo}} = 1.04 \text{ kpc}$ (Fig. 5), well inside the bulge. The retrograde motion is not unique, as a few other retrograde globular clusters exist that have endured the harsh density of the Galactic bulge (Romero-Colmenares et al. 2021; Pérez-Villegas et al. 2020; Garro et al. 2023). However, the orbit of VVV CL002 is tighter than the orbits of all other known globular clusters (Pérez-Villegas et al. 2020). No globular cluster is expected to survive over its lifetime ($>10 \text{ Gyr}$) in such proximity to the Galactic centre (Gnedin et al. 2014).

In order to unveil the mysterious history of this cluster, its chemical abundance plays an essential role. The abundances of the two stars agree within the errors, giving an estimate of the cluster metallicity of $[\text{Fe}/\text{H}] = -0.54 \pm 0.27$, which is consistent with a previous photometric determination ($[\text{Fe}/\text{H}] = -0.4$;

Moni Bidin et al. 2011), and $[\alpha/\text{Fe}] \approx +0.4$ (Table 1). The high α enhancement is connected to rapid chemical evolution dominated by core-collapse supernovae rather than type Ia supernovae (Sharma et al. 2021). This confirms that VVV CL002 is an old globular cluster formed together with other clusters and field stars present today in the Galactic bulge (Fig. 6), rather than a younger open cluster or the remains from an (already disrupted) dwarf galaxy (Hughes et al. 2020). Furthermore, using a state-of-the-art technique to estimate stellar birth radii (R_{birth}) within the Galaxy (Minchev et al. 2018), recent studies demonstrated that stars with relatively low metallicity (among bulge stars) and high α enhancement were formed predominantly in the outer parts of the Galaxy, that is, with R_{birth} of 3–6 kpc (Lu et al. 2022; Ratcliffe et al. 2023). This leads us to suggest a scenario where VVV CL002 was formed at a relatively large R_{birth} and has

recently started to fall towards the centre. This cluster is probably doomed to continue spiralling into the inner parsecs before being destroyed in the not-so-distant future. This cluster sheds light on the intriguing survival and migration mechanisms of globular clusters, whereas many less-characterised globular clusters and candidates are within a couple of kiloparsecs from the centre. Demand is high for NIR high-resolution spectroscopy of such clusters, which has so far been hampered by severe interstellar extinction.

Acknowledgements. This paper is based on the WINERED data gathered with the 6.5 meter Magellan Telescope located at Las Campanas Observatory, Chile. This research is supported by JSPS Bilateral Program Number JPJSBP120239909. The observing run in 2023 June was partly supported by KAKENHI (grant No 18H01248). We also acknowledge Scarlet S. Elgueta and Rogelio R. Albarracín for supporting the observations. WINERED was developed by the University of Tokyo and the Laboratory of Infrared High-resolution Spectroscopy, Kyoto Sangyo University, under the financial support of KAKENHI (Nos. 16684001, 20340042, and 21840052) and the MEXT Supported Program for the Strategic Research Foundation at Private Universities (Nos. S0801061 and S1411028). We gratefully acknowledge the use of data from the ESO Public Survey program IDs 179.B-2002 and 198.B-2004 taken with the VISTA telescope and data products from the Cambridge Astronomical Survey Unit. D.M. acknowledges support by the ANID BASAL projects ACE210002 and FB210003, by Fondecyt Project No. 1220724, and by CNPq/Brazil through project 350104/2022-0. J.G.F.-T. acknowledges support provided by Agencia Nacional de Investigación y Desarrollo de Chile (ANID) under the Proyecto Fondecyt Iniciación 2022 Agreement No. 11220340, and from the Joint Committee ESO-Government of Chile 2021 under the Agreement No. ORP 023/2021, and from Becas Santander Movilidad Internacional Profesores 2022, Banco Santander Chile. R.K.S. acknowledges support from CNPq/Brazil through projects 308298/2022-5 and 350104/2022-0. E.R.G. acknowledges support from ANID PhD scholarship No. 21210330.

References

- Abdurro'uf, Accetta, K., Aerts, C., et al. 2022, *ApJS*, **259**, 35
- Arca-Sedda, M., & Capuzzo-Dolcetta, R. 2017, *MNRAS*, **471**, 478
- Barbuy, B., Chiappini, C., & Gerhard, O. 2018, *ARA&A*, **56**, 223
- Barbuy, B., Cantelli, E., Muniz, L., et al. 2021, *A&A*, **654**, A29
- Baumgardt, H., & Makino, J. 2003, *MNRAS*, **340**, 227
- Borissova, J., Chené, A. N., Ramírez Alegría, S., et al. 2014, *A&A*, **569**, A24
- Carretta, E., Bragaglia, A., Gratton, R., & Lucatello, S. 2009, *A&A*, **505**, 139
- Dias, B., Barbuy, B., Saviane, I., et al. 2016, *A&A*, **590**, A9
- Fernández-Trincado, J. G., Beers, T. C., Barbuy, B., et al. 2022, *A&A*, **663**, A126
- Fukue, K., Matsunaga, N., Kondo, S., et al. 2021, *ApJ*, **913**, 62
- Garro, E. R., Fernández-Trincado, J. G., Minniti, D., et al. 2023, *A&A*, **669**, A136
- Geisler, D., Villanova, S., O'Connell, J. E., et al. 2021, *A&A*, **652**, A157
- Genzel, R., Eisenhauer, F., & Gillessen, S. 2010, *Rev. Mod. Phys.*, **82**, 3121
- Ghez, A. M., Salim, S., Weinberg, N. N., et al. 2008, *ApJ*, **689**, 1044
- Gnedin, O. Y., & Ostriker, J. P. 1997, *ApJ*, **474**, 223
- Gnedin, O. Y., Ostriker, J. P., & Tremaine, S. 2014, *ApJ*, **785**, 71
- Hughes, M. E., Pfeffer, J. L., Martig, M., et al. 2020, *MNRAS*, **491**, 4012
- Ikeda, Y., Kondo, S., Otsubo, S., et al. 2022, *PASP*, **134**, 015004a
- Kunder, A., Pérez-Villegas, A., Rich, R. M., et al. 2020, *AJ*, **159**, 270
- Leon, S., Meylan, G., & Combes, F. 2000, *A&A*, **359**, 907
- Lu, Y., Minchev, I., Buck, T., et al. 2022, *Nat. Lett.*, submitted, [arXiv:2212.04515]
- Matsunaga, N., Fukue, K., Yamamoto, R., et al. 2015, *ApJ*, **799**, 46
- Matsunaga, N., Taniguchi, D., Elgueta, S. S., et al. 2023, *ApJ*, **954**, 198
- Mészáros, S., Masseron, T., García-Hernández, D. A., et al. 2020, *MNRAS*, **492**, 1641
- Minchev, I., Anders, F., Recio-Blanco, A., et al. 2018, *MNRAS*, **481**, 1645
- Minniti, D., Fernández-Trincado, J. G., Smith, L. C., et al. 2021, *A&A*, **648**, A86
- Moni Bidin, C., Mauro, F., Geisler, D., et al. 2011, *A&A*, **535**, A33
- Moreno, E., Fernández-Trincado, J. G., Pérez-Villegas, A., Chaves-Velasquez, L., & Schuster, W. J. 2022, *MNRAS*, **510**, 5945
- Murali, C., & Weinberg, M. D. 1997, *MNRAS*, **288**, 749
- Navarro, M. G., Capuzzo-Dolcetta, R., Arca-Sedda, M., & Minniti, D. 2023, *A&A*, **674**, A148
- Pérez-Villegas, A., Barbuy, B., Kerber, L. O., et al. 2020, *MNRAS*, **491**, 3251
- Queiroz, A. B. A., Chiappini, C., Perez-Villegas, A., et al. 2021, *A&A*, **656**, A156
- Queiroz, A. B. A., Anders, F., Chiappini, C., et al. 2023, *A&A*, **673**, A155
- Ratcliffe, B., Minchev, I., Anders, F., et al. 2023, *MNRAS*, **525**, 2208
- Recio-Blanco, A. 2018, *A&A*, **620**, A194
- Romero-Colmenares, M., Fernández-Trincado, J. G., Geisler, D., et al. 2021, *A&A*, **652**, A158
- Sanders, J. L., Smith, L., & Evans, N. W. 2019, *MNRAS*, **488**, 4552
- Schiavon, R. P., Phillips, S. G., Myers, N., et al. 2024, *MNRAS*, **528**, 1393
- Schultheis, M., Rojas-Arriagada, A., Cunha, K., et al. 2020, *A&A*, **642**, A81
- Sharma, S., Hayden, M. R., & Bland-Hawthorn, J. 2021, *MNRAS*, **507**, 5882
- Taniguchi, D., Matsunaga, N., Kobayashi, N., et al. 2018, *MNRAS*, **473**, 4993
- Zasowski, G., Schultheis, M., Hasselquist, S., et al. 2019, *ApJ*, **870**, 138